Progress In Electromagnetics Research C, Vol. 64, 125–132, 2016

Compact 30:1 Bandwidth Ratio Balun for Printed Balanced Antennas

Xueqing Meng, Bo Wu, Zhixiang Huang*, and Xianliang Wu

Abstract—A new compact 30 : 1 bandwidth ratio balun and its application to balanced antennas are presented in this paper. To realize the balun-type function, two different types of wideband transition structures are adopted for unbalanced and balanced outputs of the balun. Further, a Vivaldi antenna integrated with the proposed balun is designed and fabricated to validate the feasibility of the new approach. Results indicated that the proposed balun can operate from 0.2 GHz to 6 GHz (a bandwidth ratio of 30 : 1). And it exhibits a good balanced performance within 0.5 dB magnitude imbalance and less than 6 degree phase imbalance between the two balanced outputs. In addition, the antenna can operate from 0.9 GHz to 6 GHz with good unidirectional radiation patterns.

1. INTRODUCTION

Nowadays, compact and low cost wireless communication systems are under growing demands. Therefore, the demand for microwave antennas with highly desirable properties (such as compact size, low profile, ultra-wideband, and etc) has been developed rapidly. The balanced antennas, such as Vivaldi antennas, are widely used in many applications due to its broad bandwidth, low profile, low cross polarization, and perfect directive radiation performance. Unfortunately, the balanced antennas must be excited through differential driving circuits. Balun is an important component used for single and differential signal transition. It can not only convert an unbalanced input single-ended signal into its balanced differential ones but also realize impedance matching. Therefore, research on wideband high performance balun is meaningful for RF frond-ends. Over the past few years, much effort has been focused on this area [1–16].

In order to reduce the circuit dimension, baluns based on low-temperature co-fired ceramic (LTCC) technology and COMS technologies were presented in [1–3], respectively, yet the multilayer process increases the complexity and the cost of the circuits. By combining the lumped element and microstrip line, lumped-element baluns were introduced with compact size in [4] and [5], while they could not realize wide bandwidth due to inherent characteristic of lumped elements. Based on microstrip Marchand balun prototype, baluns with good performance [6–9] have been designed. On the other hand, several wideband baluns using coupled lines were introduced in [10, 12]. To further wider the operation bandwidth, baluns utilizing the technology of filed transformation structures have been received much attention [13–16]. However, the baluns presented in above works can not meet the requirement of compact size.

The primary motivation of this paper is to design a new ultra-wideband balun with compact size for printed balanced antennas. By utilizing the electric filed distribution characteristics of the two different types of transition structures, i.e., the microstrip-coplanar waveguide (CPW)-microstrip transition and the microstrip-coplanar stripline (CPS)-microstrip transition, a new ultra-wideband balun has been designed. To verify the design concept, the proposed ultra-wideband balun and its application for Vivaldi antennas are designed, fabricated, and measured. Results show that the proposed balun exhibits

Received 20 April 2016, Accepted 18 May 2016, Scheduled 28 May 2016

* Corresponding author: Zhi-Xiang Huang (zxhuang@ahu.edu.cn).

The authors are with the Key Laboratory of Intelligent Computing and Signal Processing of Ministry of Education, Anhui University, Hefei 230039, China.

wide operation band and a good amplitude/phase imbalance between the balanced outputs. Meanwhile, the antenna integrated with the new balun reveals good unidirectional radiation patterns.

2. CIRCUIT DESIGN

2.1. Ultra-Wideband Balun Design

The top view of the proposed balun is shown in Fig. 1. It consists of a T-junction power divider and two different types of transition structures. The two transitions are a microstrip to coplanar waveguide (CPW) transition and a microstrip to coplanar stripline (CPS) transition, and they are defined as the transition structure I and II, respectively. Specifically, the transition structure I is realized by connecting the microstrip lines to the CPW through short-ended via holes. And the transition structure II is realized by introducing shorting pins between the microstrip lines and the CPS. It is worthy mentioning that these two transition types adopted here are to achieve wideband phase and magnitude balance performance. As can be seen from Fig. 1, when an incident signal is fed at port 1 it will be divided into two identical signals by the T-junction power divider. After the two signals transmitting through the transition structure I and transition structure II simultaneously, a balanced performance can be achieved between two balanced ports, i.e., ports 2 and 3.

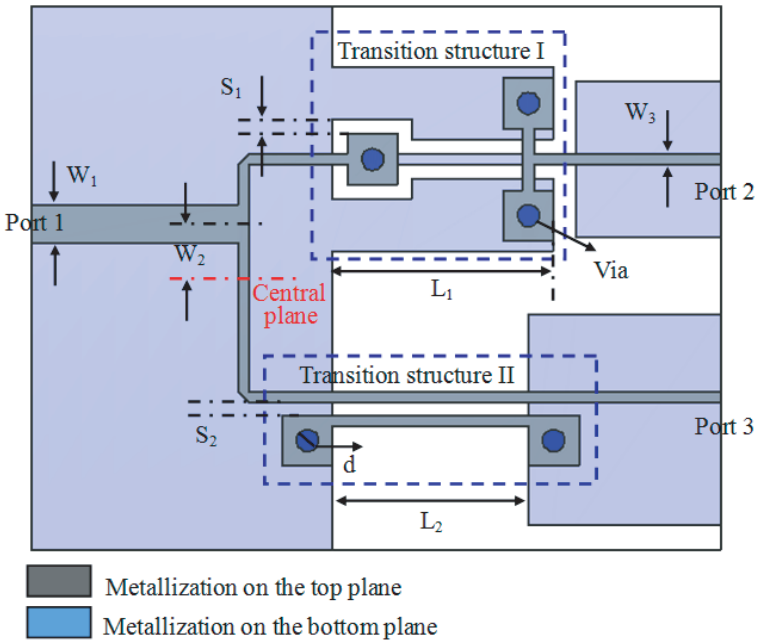

Figure 1. Top view layout of the proposed balun.

The viewpoint of electronic filed distributions can be used to explain the working principles of these two transitions. The electronic filed distributions in different cross sections are described as shown in Fig. 2 and Fig. 3. When the two identical signals are excited from the two output ports of the T-junction power divider, they will go through the transition I and the transition II, respectively. Comparing the electric field distributions in different cross sections, we can find that the electric field lines at the 1-1 and 1'- 1' sections are same. Then, the signals go through different transition structures, the electric field distributions will undergo different variations as shown in Fig. 2(b) and Fig. 3(b). Finally, the electric field lines at the 5-5 and 5'-5' sections are opposite. It means an 180° phase difference between the 5-5 section and 5'-5'section. Therefore, after introducing the two transitions, the phase difference between the signals at the two outputs will be out of phase. It should be mentioned that, due to the inherent wideband character of the two transitions, the proposed scheme here is able to achieve excellent phase and amplitude balance performance in wide band.

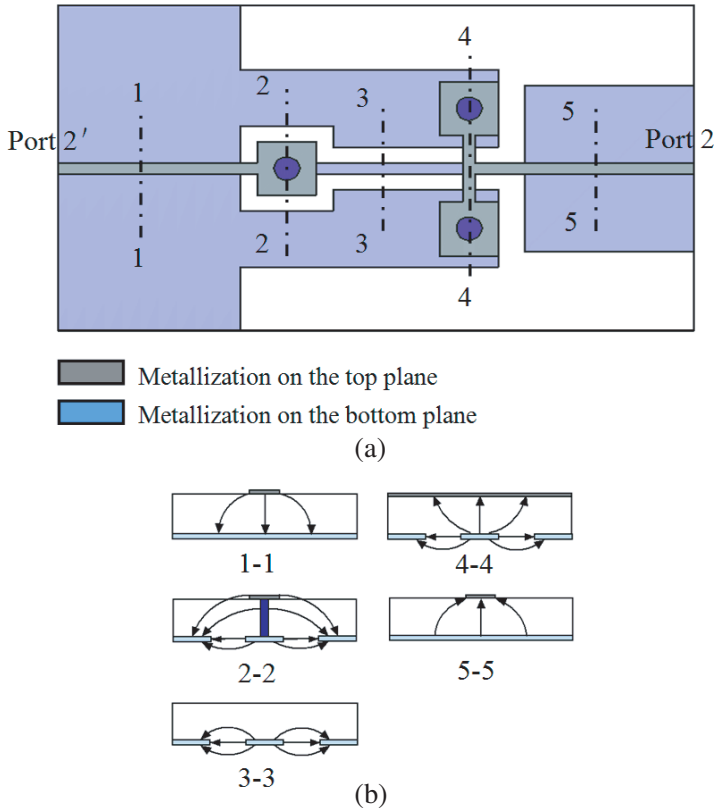

Figure 2. (a) Configuration of transition I and (b) electric filed lines at various cross planes of the structure.

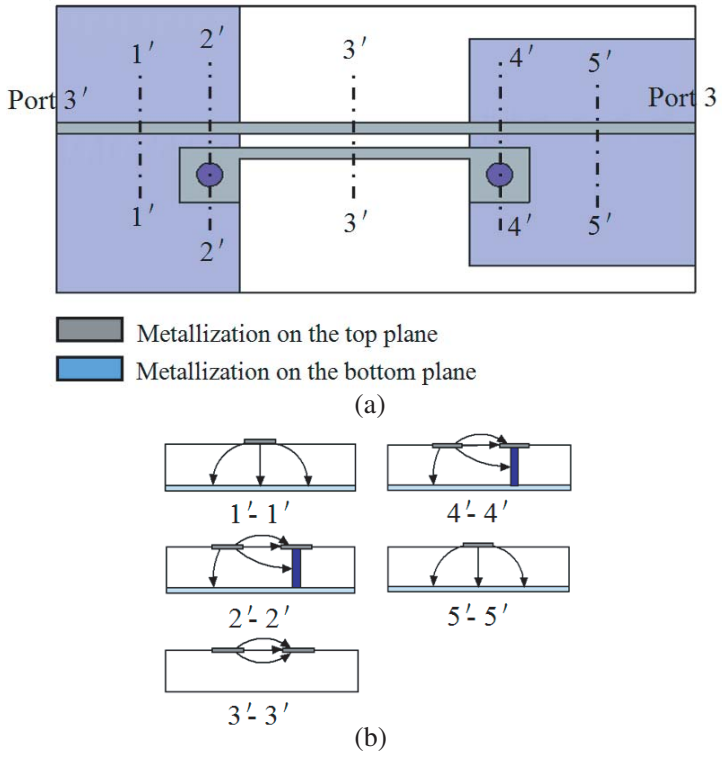

Figure 3. (a) Configuration of transition II and (b) electric filed lines at various cross planes of the structure.

To verify the design concept, the proposed balun is designed and fabricated on a single layer printed circuit board (PCB). The substrate used here has a dielectric constant of 3.38, a loss tangent of 0.0027, and a thickness of 0.508 mm. It is worthy mentioning that the characteristic impedance of the two output microstrip lines is around 75 Ω to meet the impedance of the balanced antenna. For that reason, the value of the two output microstrip lines impedance is 75 Ω. The dimensions of proposed ultra-wideband balun are presented in Table 1. The balun has been analyzed and the simulation was accomplished by the EM simulator HFSS while the measurement was carried out on an Agilent N5244A network analyzer. The simulated and measured results of the phase imbalance and magnitude imbalance are shown in Fig. 4. It can be seen that the balun has achieved a bandwidth ratio of 30 : 1 (operates from 0.2 GHz to 6 GHz). Along the whole bandwidth, the measured in-band insertion loss is less than 1 dB with the return loss better than 14 dB. It can also be found that better than 0.5 dB amplitude imbalance and 180° ± 5° phase difference are both achieved.

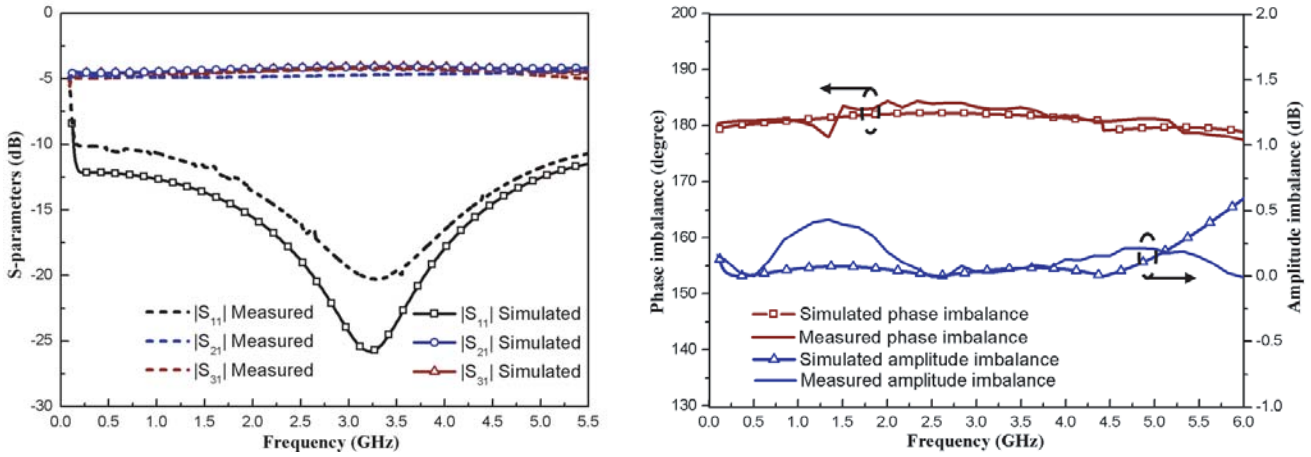

(a) (b)

Figure 4. Simulated and measured S-parameter and amplitude and phase imbalance. (a) S-parameter, (b) amplitude and phase imbalance.

2.2. Balanced Antenna Design

To further verify the feasibility of the design concept, the balun is utilized to feed a Vivaldi antenna. The configuration of proposed balun integrated with balanced antenna is shown in Fig. 5. The Vivaldi antenna consists of two symmetrically exponential tapered patches which are connected to the two balanced outputs of the balun respectively. The inner and outer edges of the tapered patches are designed as

$$y_i = \pm((\exp(30 \cdot x) - 1000)/400 + s/2) \quad (1)$$

$$y_o = \pm((\exp(70 \cdot y) - 1000)/650 + s/2 + w4) \quad (2)$$

where y_i and y_o represent the inner and outer edges of the tapered patches, respectively.

When the adopted Vivaldi antenna is excited by the balun, multiple current paths could be realized on the two exponential tapered patches. Thus, the adopted antenna could be able to achieve wideband radiation performance. The impedance matching between the outputs of balun and the tapered patches also has a significant effect on the performance of the adopted antenna. For the designed antenna, the exponential tapered patches can be regard as a load of the proposed balun. Since the impedance of balanced antenna without balun is around 150 Ω. And the impedance of the balanced outputs is around 75 Ω. For that reason, the characteristic impedance of output microstrip lines of the proposed balun can well meet the impedance matching.

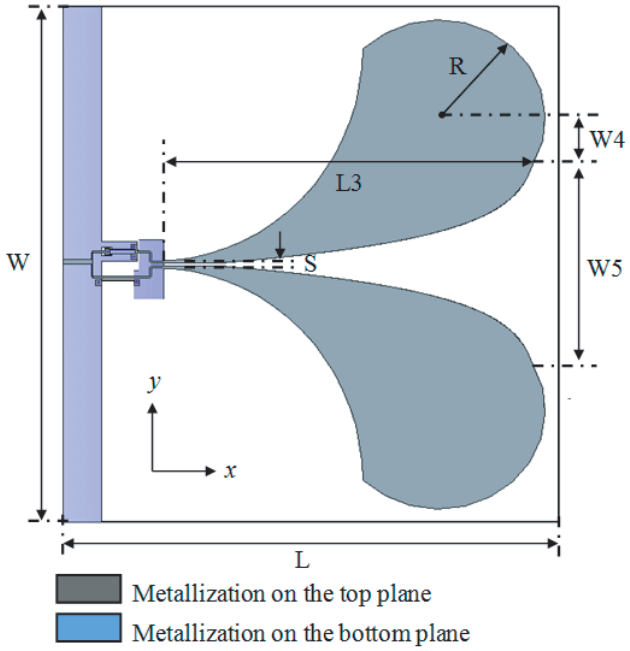

Figure 5. Configuration of the proposed Vivaldi antenna.

3. SIMULATION AND MEASUREMENT RESULTS

The proposed balanced antenna is fabricated with its photograph shown in Fig. 6. The dimensions of the Vivaldi antenna are presented in Table 2. The substrate used here has a dielectric constant of 3.38, a loss tangent of 0.0027, and a thickness of 0.508 mm. Fig. 7 shows the simulated and measured results of the scattering parameters. Simulation was accomplished by the EM simulator HFSS while the measurement was carried out on an Agilent N5244A network analyzer. The simulated and measured results are in good agreement. As can be seen, the measured impedance bandwidth, defined by S_{11} lower than -10 dB, is from 0.9 GHz to 6 GHz. The results prove the feasibility of the proposed design. The gain and radiation patterns at different frequencies are also measured by employing a Microwave Vision Group's Starlab near-field antenna measurement system. The measured gain is depicted in Fig. 8, with

(a) (b)

Figure 6. Photograph of the fabricated antenna. (a) Top view, (b) bottom view.

the simulated one for comparison. It should be mentioned that the discrepancy between measured and simulated results are mainly due to the fabrication error and measurement error. It can be seen that the measured gain is better than 4.5 dB in the operating band. The minimum gain is 4.7 dB at 1.25 GHz, and maximum gain is 8.1 dB at 6 GHz.

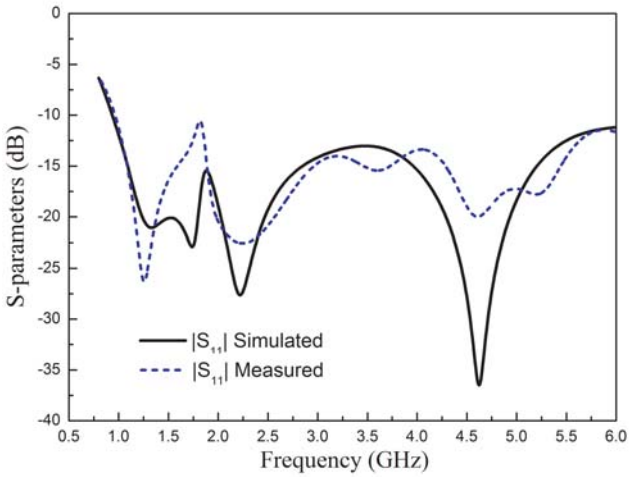

Figure 7. Simulated and measured reflection coefficient of the proposed antenna.

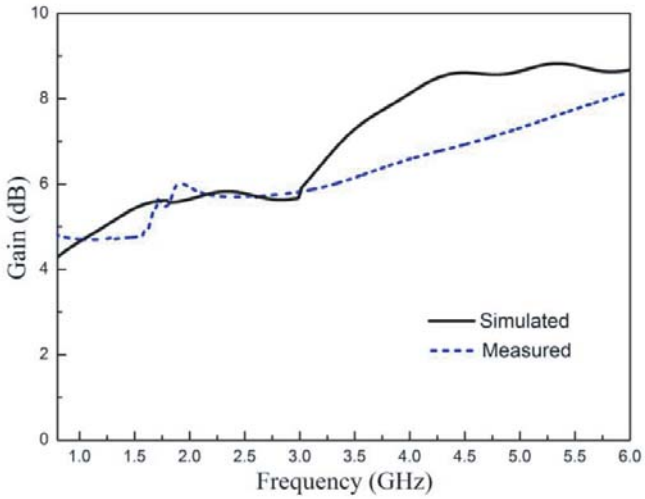

Figure 8. Simulated and measured gains of the proposed antenna.

Table 1. Geometrical parameters of the designed balun (unit: mm).

W_1	W_2	W_3	L_1	L_2	S_1	S_2	d
1.05	1.5	0.3	4.9	4.2	0.4	0.17	0.6

Table 2. Dimension values of the proposed antenna (unit: mm).

W	W_4	W_5	L	L_3	S	R
133	15	52.3	117.5	88	0.95	22

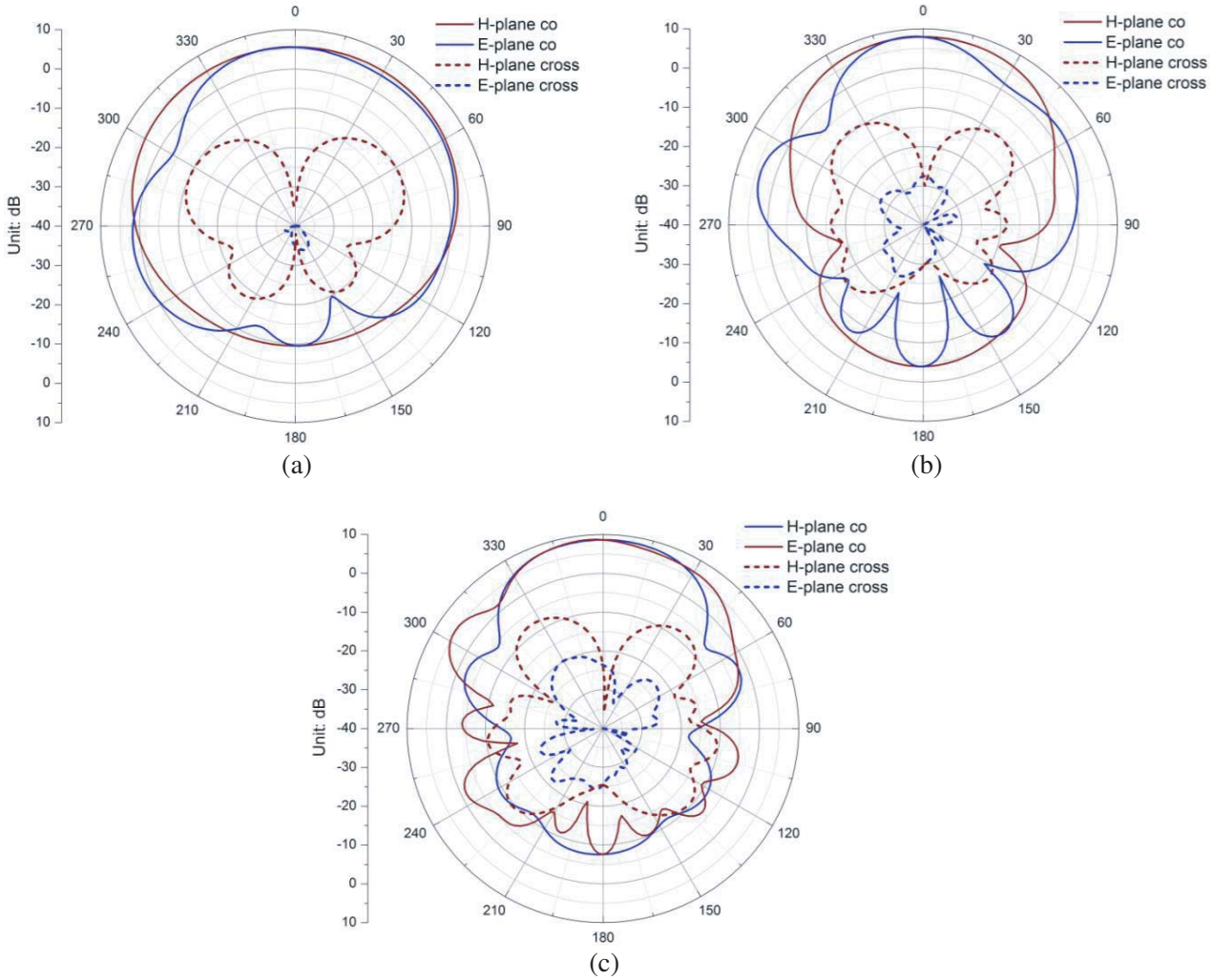

Figure 9. Measured radiation patterns of the proposed printed Vivaldi antenna in E-plane (xoy-plane) and H-plane (xoz-plane) at different frequencies. (a) 2 GHz, (b) 4 GHz, (c) 6 GHz.

Figure 9 shows the measured far-field radiation patterns in E-plane (xoy-plane) and H-plane (xoz- plane) at 2 GHz, 4 GHz, and 6 GHz. It is observed that the proposed antenna reveals good unidirectional radiation patterns in the E- and H-planes. Specifically, within the passband, settled radiation directivity is achieved and the main lobes of the radiation patterns are fixed in x-axis direction. Stable radiation directivity is achieved. In addition, the simulated and measured cross-polarization of the Vivaldi antenna is also presented in Fig. 9. It is apparent from the plots that the antenna has very low cross-polarization values which are nearly 20 dB below than the co-polarization values in the direction of maximum radiation. It should be mentioned that the small discrepancy between measured and simulated results are mainly due to the fabrication tolerance. Overall, the Vivaldi antenna fed by proposed balun has good radiation performance in a wide band.

4. CONCLUSION

In this paper, a new 30 : 1 bandwidth ratio balun and its application to wideband balanced antennas have been presented. To verify the feasibility of the design concept, a Vivaldi antenna integrated with the proposed balun has been designed, fabricated, and measured. Results indicate that the demonstrator exhibits the properties of wideband, good radiation performance and very low cross-polarization. We

believe the proposed balun will be suitable for many applications, such as push-pull amplifiers circuits and wideband balanced antennas.

ACKNOWLEDGMENT

The work was supported by the NSFC (Nos. 61471001, 51277001), Natural Science Foundation of Anhui Province (Nos. KJ2012A013, 1508085JGD03, 1508085QF130), DFMEC (No. 20123401110009) and NCET (NCET-12-0596) of China.

REFERENCES

1. Guo, Y. X., Z. Y. Zhang, L. C. Ong, and M. Y. W. Chia, "A novel LTCC miniaturized dualband balun," *IEEE Microw. Wireless Compon. Lett.*, Vol. 16, No. 3, 143–145, 2006.
2. Suh, B., Y. Kim, T. Kim, and S. Jeon, "K- and Ka-band miniature CMOS balun with a single spiral coupled structure," *Journal of Electromagnetic Waves and Applications*, Vol. 27, No. 15, 1910–1918, 2013.
3. Chiou, H. K. and J. Y. Lin, "Balanced mixers using wideband symmetric offset stack balun in 0.18 μm CMOS," *Progress In Electromagnetics Research C*, Vol. 23, 41–54, 2011.
4. González-Posadas, V., C. Martín-Pascual, J. Luis Jiménez-Martín, and D. Segovia-Vargas, "Lumped-element balun for UHF UWB printed balanced antennas," *IEEE Transactions on Antennas and Propagation*, Vol. 56, No. 7, 2102–2107, 2008.
5. Ye, Y., L. Y. Li, J. Z. Gu, and X. W. Sun, "A band width improved broadband compact lumped-element balun with tail inductor," *IEEE Microw. Wireless Compon. Lett.*, Vol. 23, No. 8, 415–417, 2013.
6. Yang, Z. Q., T. Yang, and Y. Liu, "Analysis and design of a reduced-size Marchand balun," Vol. 21, No. 9, 1169–1175, 2007.
7. Kian, S. A. and D. R. Ian, "Analysis and design of impedance-transforming planar Marchand baluns," *IEEE Trans. Microw. Theory Tech.*, Vol. 49, No. 2, 402–406, 2001.
8. Ma, Q., B.-H. Sun, J.-F. Li, and Q.-Z. Liu, "A differential rectangular patch antenna with Marchand balun for UWB applications," *Journal of Electromagnetic Waves and Applications*, Vol. 23, No. 1, 49–55, 2009.
9. Bai, S., W. Feng, and W. Che, "Compact wideband differential bandpass filter using a Marchand balun," *Progress In Electromagnetics Research C*, Vol. 53, 67–73, 2014.
10. Jafari, E., F. Hodjatkashani, and R. Rezaiesarlak, "A wideband compact planar balun for UHF DTV applications," *Journal of Electromagnetic Waves and Applications*, Vol. 23, No. 14–15, 2047–2053, 2009.
11. Abbosh, A., "Ultra-wideband quasi-Yagi antenna using dual-resonant driver and integrated balun of stepped impedance coupled structure," *IEEE Transactions on Antennas and Propagation*, Vol. 61, No. 7, 3885–3888, 2013.
12. Chen, C. M., S. J. Chang, Y. L. Pan, C. Y. Chen, and C. F. Yang, "Fabrication of compact microstrip line-based balun-bandpass filter with high common-mode suppression," *International Journal of Antennas and Propagation*, Vol. 2014, Article ID 985064, 6 pages, 2014.
13. Shao, J., R. Zhou, C. Chen, X. H. Wang, H. Kim, and H. Zhang, "Design of a wideband balun using parallel strips," *IEEE Microw. Wireless Compon. Lett.*, Vol. 23, No. 3, 125–127, 2013.
14. Sánchez, A. M., M. Ribó, L. Pradell, J. Anguera, and A. Andújar, "CPW balun for printed balanced antennas," *Electron. Lett.*, Vol. 50, No. 11, 785–786, 2014.
15. Hong, Y. P., "Fat dipole antenna with broadband balun using CPW-to-slotline field transformation," *Electron. Lett.*, Vol. 49, No. 10, 635–636, 2013.
16. Lin, S.-C., T.-L. Jong, C.-W. Hsieh, and K.-J. Ho, "Wideband series-fed dipole antenna with balun integrated," *Journal of Electromagnetic Waves and Applications*, Vol. 24, No. 17–18, 2463–2477, 2010.